

# Effect of the Fractal-Grid Generated Turbulence on Turbulent Intensity and Pressure Drop in Pipe Flow

Mohd Hanafi Lahadi<sup>1,\*</sup>, Annizar Mohd Johari<sup>2</sup>, Zainal Abidin Alias<sup>3</sup>

<sup>1</sup> EMFA Industry Sdn Bhd, PT.7457 Batu 2½, Jalan Air Putih, 24000 Kemaman, Terengganu, MALAYSIA,

<sup>2</sup> Nukilan Gemilang Sdn Bhd, No. 3, Lorong Seri Teruntum 36, Seri Teruntum, 25100 Kuantan, Pahang, MALAYSIA

<sup>3</sup> Aeronautical Laboratory, Faculty of Mechanical and Manufacturing Engineering, Universiti Tun Hussein Onn Malaysia, MALAYSIA

Received 26 September 2018;  
Accepted 01 January 2019;  
Available online 02 February  
2019

**Abstract:** The orifice plate flow meter is the most common form of differential pressure flow meter used in industry. However, in practical applications the flow approaching the orifice meter is often disturbed by pipe-fittings and consequently the measurements become inaccurate. Basically, the design of orifice plate meters that are independent of the upstream disturbances is a main goal for orifice plate metering. Either using a long straight pipe, or a flow conditioner upstream of an orifice plate, usually achieves this goal. This paper will discuss the effect of the fractal flow conditioner flow conditions has been investigated in an experimental rig and validation of the results has been justified with the appropriate CFD domains. Experiments will be conducted in transparent pipe for easy to see the change of the air flow after across the fractal conditioner. These experiments will be run at five times using three different porosity fractal plates. Two methods will be used for velocity measurements which are using Pitot tube to measure inlet velocity and hot wire anemometer to measure mean velocity fluctuations within the test section. Experimental result will be presented in form of velocity profiles as well as the velocity fluctuations due to the traverse distance from y-axis. Whole the results will lead to the objectives of this case study whether achievable or not and as an alternative to the measurement of turbulent intensity.

**Keywords:** CFD, flow meter, fractal plate, orifice

## 1. Introduction

Turbulent premixed flames are of great important for technical combustion systems as they can produce high power densities and low pollutant emissions at the same times. Within this framework, the impact of turbulent flow field characteristic on different flame properties, such as the turbulent burning velocity is of great interest for combustion research. Standard turbulence generating grids, such as perforated plate are normally used for non-swirl stabilized flames to ensure a well develop velocity field. Although normal grids can generated high levels of turbulence near to grid, the turbulence decays quickly further downstream of the grid, and as a consequence, the resulting flames are exposed to a rather low turbulence.

In comparison to a diffusion flame, carbon and soot particles formed in a premixed flame also meet the oxidizer within a flame and react with them. As a result, small soot particles and lower mass output are generally expected from a premixed flame [1]. Obviously, the soot particles and the mass output will grow when the oxygen content in the fuel gas reduces and the flame becomes a diffusion flame. In combustion, a diffusion flame is a flame in which the oxidizer,

in our case the oxygen in the air combines with the fuel by diffusion [2]. As a result, the flame speed is limited by the rate of diffusion. Diffusion flames tend to burn slower and to produce more soot than premixed flames because there is not sufficient oxidizer within the flame.

### 1.1 Background of Study

Turbulent premixed flames are of great important for technical combustion systems as they can produce high power densities and low pollutant emissions at the same times. Within this framework, the impact of turbulent flow field characteristic on different flame properties, such as the turbulent burning velocity is of great interest for combustion research [3]. Standard turbulence generating grids, such as perforated plate are normally used for non-swirl stabilized flames to ensure a well develop velocity field. Although normal grids can generated high levels of turbulence near to grid, the turbulence decays quickly further downstream of the grid, and as a consequence, the resulting flames are exposed to a rather low turbulence.

Due to the background of study, the objectives of this study are to ascertain a new approach in turbulence generators

on the turbulent intensity and pressure drop using a fractal-grid pattern. Besides that, the capability of the fractal grid pattern in mixing process will be determine. At the end of this research, recommendations for new concept of static mixer in burner combustion by using fractal concept based on space filling circle grids fractal will be approach.

**1.2 Fractal Concept**

The world around us is not naturally smooth-edged; it consists of rough edges on small scales. This fact has been addressed from long time ago and described on mathematical foundation in the year 1975, when a mathematician Mandelbrot assigned the word “fractal” to describe such that non-smooth edged shapes of self-similar characteristics or irregular shapes, he took the word from the Latin word “fractus”, which means broken or discontinuous features.

Since that time, fractals have been received more attention due to their graphic art potential in describing some complicated shapes, for example: mountains, clouds and landscapes, in fact most computers graphic techniques actually employ a stochastic approximation of true fractal functions. Fractal geometry can be defined as the geometry of irregular shapes where an identical pattern repeats itself on an ever diminishing scale [3]. The fractal geometry is an extension of the classical geometry but does not replacing it, it enhances its usage. The geometrical figure can be for example a square, a hexagon, a rectangular, a triangle shape or even circular shape.

**2. Previous Work on Flow through Fractal**

There are limited experimental studies are available on fractal patterns in flow measuring due to the complexities in manufacturing and the associated difficulties in the setup process and control of the measured flow parameter. Accordingly, the fractal generated turbulence has progressed slowly for the same reasons. One of the applications of fractal shaped objects in industry has been concentrated on distributing the fluid in the molasses chromatography process for controlling exhaustion in thin juice ion exchange and for providing uniform air circulation in a sugar silo [4]. Their increasing role is based on their rapid mixing, controlled formation of specified fluid geometry and due to their low energy fluid distribution.

In a study of fractal generated turbulence [5], a shell model for fractal dimension objects was introduced. In this research, it was found that the power of the shell-model fractal forcing is an increasing function of the fractal dimension of the fractal object. Also, their results were sensitive to the modeling of the fractal forcing, but overall supported the idea that the fractal forcing can be expected to change the turbulence scaling properties. Other researchers [6] investigated experimentally the scaling properties of the turbulent wake after three dimensional fractal grids in a wind tunnel. As a result, the scaling properties of the turbulence, as the turbulence intensity, are depending on the orientation and the position of the fractal object relative to the velocity sensors.

Previous work by the Sheffield group using a Koch snowflake fractal pattern has been conducted in small wind tunnel [7]. In order to investigate a pressure drop after a fractal shaped orifice in turbulent pipe flow, they found that the fractal-shaped orifices have significant effect on the flow downstream the flow and enhance the mixing properties leading to this pressure drop reduction. Also the results showed that with the increase of the fractal shaped orifice generation, the differences between the pressure drop from the fractal-shaped orifices and that from the regular orifices increased until

reach the fourth generation when the pressure drop reduces again. It indicates that with the increase of producing finer fractal-shaped orifice edges, it will approximately reach the characteristics of the ordinary orifices.

**3. Experimental Facilities and Testing Methods**

To assess the effect fractal flow conditioners on the orifice plate flow meter, one experimental facility have been built that is air test rig. In these facilities, the mass flow rate of the orifice plate with both standard and non-standard velocity profiles have been examined for different Reynolds number and  $\beta$  ratio. In the air test rig, air was used as the working fluid at a relatively low Reynolds number which varied from 7917 to 11528. For air test rigs an orifice plate with  $\beta$  ratio of 0.38, 0.5, and 0.7 was used in the pipes.

**3.1 Air Test Rig**

The air test rig was used to measure the pressure difference across the fractal plate and also the turbulence intensity of the flow downstream. The air test rig was a conventional type of open circuit tunnel with a cross sectional area of 0.00196 m<sup>2</sup> and a total length of 3.125 m. The inlet velocity was measured by a pitot tube located 11.5D downstream of the pipe entrance. A schematic diagram of the air test rig is shown in Fig. 1.

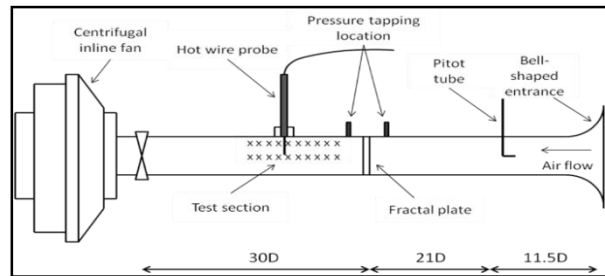


**Fig.1 - Schematic diagram of the air test rig**

The instantaneous velocity measurements were made at different locations downstream after passing through fractal plate using hot wire anemometry. The flow was characterized using mean velocity profile  $U_{mean}$ , RMS deviation from the mean  $U_{rms}$  and turbulent intensity  $T_i$ . The equations for these parameters are given in Eqn. 1 to 3 below, where  $N$  is the number of samples, and  $U_i$  is an instantaneous velocity measurement.

$$U_{mean} = \frac{1}{N} \sum_1^N U_i \tag{1}$$

$$U_{rms} = \left( \frac{1}{N-1} \sum_1^N (U_i - U_{mean})^2 \right)^{0.5} \tag{2}$$

$$T_i = \frac{U_{rms}}{U_{mean}} \tag{3}$$

During the experiment, the flow was driven by a centrifugal inline fan with a speed controller. A bell mouth was used at the inlet of the pipe to ensure that the flow was fully developed in a short distance. To measure the pressure difference across the fractal plate, two pressure tapping were used,  $D$  upstream and  $D/2$  downstream of the fractal plate. The pressure tapping were connected to a digital micro-manometer (Testo 510) using plastic tubing. The pressure drop was also measured, using liquid-filled differential manometers to ensure the accuracy of the data. As the flow rates were calculated using the density of the air, the atmospheric pressure and temperature were measured for each set of experiments.

### 3.2 Experimental Works

In the experimental work using the air test rig, the centerline flow velocities were examined. The axial mean, fluctuation (RMS) velocity and turbulent intensity 2 to 10 diameters downstream of the metal foam flow conditioners were measured using hot wire anemometry. The measurements were taken every 2.5cm (1/2 pipe diameter) starting from 1D to 8D downstream of the fractal plate. Every point will be taken 10 measurements that are from center to the wall of pipe and the distance between the points is 3mm. Fig.2 shows detail position fractal plate and test section. These tests were conducted at difference Reynolds number that is 11528, 10625, 9722, 8819, and 7917.

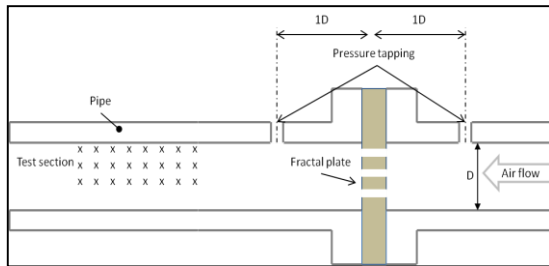


**Fig. 2 - Drawing position fractal plate in pipe and pressure tapping**

Axial turbulence intensity measurements were made using a single hot-wire-anemometer probe made of tungsten. The probe was positioned in the test rig using a radial traversing mechanism incorporating a linear scale which allowed the radial position of the probe to be adjusted to an accuracy of  $\pm 0.5$  mm. A typical RMS error on the calibration curve was around  $0.1 \text{ ms}^{-1}$ .

### 3.3 Sources of Errors in Metering

Basically every meter involves some kind of error. In the flow metering domain these errors affect the accuracy, uncertainty and the various other parameters described in the previous chapter. Hence, the identification and reduction of possible errors in metering is a key part of this investigation. Essentially there are four types of errors in metering [9] known as: spurious errors, random errors, constant or systematic errors and variable systematic errors.

Spurious errors are caused by obvious failure or instrument malfunction. This error can be avoided by following the manufacturer's instructions and warnings. Random errors are caused by different mechanics, most of the time unknown. The result is that the output reading is changed even when the input parameters are kept constant. The constant error is constant with time or may change over the range of metering and is then known as a systematic error. Finally the variable systematic can be made by wear and fatigue in components of metering or erosion of the geometry this last one varies with time.

Generally, the random errors and systematic errors are the most important parameters which affect the accuracy and uncertainty of the metering. There is no way to reduce the systematic error except by using more precise instrumentation. Random errors can be reduced by repeating the metering based on the correct process or the manufacturer's instructions. Great efforts have been taken during the experiments described here to reduce these errors by choosing precise instruments and repeating the measurement at least two or three times for each case to ensure that the results are as accurate as possible.

Finally, the most important thing regarding the measurement was that, as the same method was used for all of

the flow metering, any systematic errors could be eliminated from the results. As a result it can be concluded that the errors in metering were as low as possible, given the limitations of the scale of the rig and the types of instrumentation used.

## 4. Results and Discussion

The level of turbulence intensity in air has implications in many different fields such as in the automobile industry, the measurement of turbulence intensity is used when evaluating the aerodynamics of an auto body design. Besides that, in the realm of aeronautic the turbulence intensity also can affect fuel efficiency. In this study, it more focused on turbulence intensity and pressure drop was generated by three fractal plates that have different porosity and ratio. This chapter will show the results for three experiments in the graph form. The results just based on the experiments without compared with theoretical results.

### 4.1 Turbulence Intensity for Various Reynolds Number

As the fractal grid is conceived using the concept of creating a disturbance or level of turbulence that can absorb all the other disturbances, it is important to measure the magnitude of the turbulent wake downstream of the fractal grid. Turbulence intensity was measured by equations (1-3). Basically, turbulence intensity was measured by velocity flow of air after through the plate at different point and the measurement using hot wire anemometer.

The results show the axial turbulence intensity plotted 1D to 8D downstream of the fractal grid. There two types of graph will shows turbulence intensity based on differential of blockage ratio and Reynolds number of air. Both of the graph title is turbulence intensity versus  $x/D$  which  $x$  is distance point from fractal plate in  $x$ -axis and  $D$  is diameter of pipe. In this experiment, Pitot tube is used to measure inlet velocity of air through bell mouth. The inlet velocity of air was controlled by manual and the values have fluctuation. Because of the fluctuation, average approach taken into consideration. Pitot tube has been located at  $11.5D$  form bell mouth to make sure the flow fully developed in short distance.

**Table 1 - Reynolds number for  $x$ -axis 11.5D**

Inlet velocity (m/s)	Reynolds number
3.32	11528
3.06	10525
2.8	9722
2.54	8819
2.28	7917

For Reynolds number 11528, the inlet velocity flow of air is maximum that is 3.32m/s. The Fig. 3 shows parabolic curve which means turbulence intensity decreases when getting away from the fractal plate. At level  $x/D=1$ , the highest turbulence intensity is 0.85 that had been generated by plate  $\beta=0.38$  and the lowest is 0.44 from plate  $\beta=0.7$ . While at the farthest distance from fractal plate, the highest turbulence intensity is 0.11 generated by plate  $\beta=0.7$  and followed by plate  $\beta=0.38$  and plate  $\beta=0.5$ . Based on the graph, turbulence intensity decreases dramatically start from point  $x/D=1$  to  $x/D=4$  and then decreases to a relatively constant until point  $x/D=8$ . It means that if the distance is more far from fractal plate, plate  $\beta=0.7$  will generate higher turbulence intensity than others. Turbulence intensity was generated by plate  $\beta=0.38$  is higher than plate  $\beta=0.5$  at all point. Although plate  $\beta=0.7$  generated low turbulence intensity initially, at point  $x/D=2.6$  and  $x/D=4.6$  it generate same turbulence intensity with plate  $\beta=0.5$  and plate  $\beta=0.38$  that is 0.26 and 0.16.

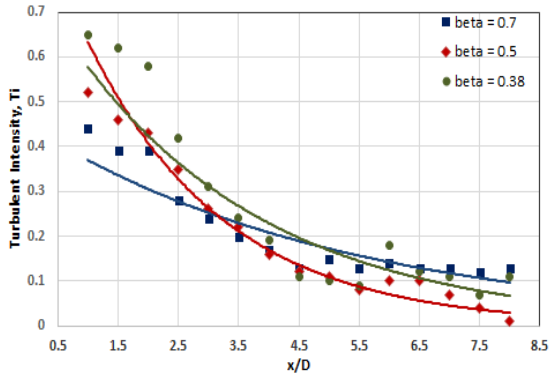


Fig. 3 - Turbulence intensity against  $x/D$  for Re number 11528

Fig. 4 shows relationship between turbulence intensity and  $x/D$  using Re number 10625 that is 3.06m/s inlet velocity of air flow. Based on the graph, turbulence intensity will decrease when it farther away from the fractal plate until it reach constant turbulence intensity. At the first point  $x/D=1$ , plate  $\beta=0.38$  generated the highest turbulence intensity that is 0.87 followed by plate  $\beta=0.5$  and plate  $\beta=0.7$ . For plate  $\beta=0.7$ , turbulence intensity is lowest at initially point but higher than plate  $\beta=0.5$  and plate  $\beta=0.38$  at point  $x/D=2$  and  $x/D=3.2$ . After point  $x/D=3.2$ , plate  $\beta=0.7$  generate turbulence intensity higher than plate  $\beta=0.5$  and plate  $\beta=0.38$  until the end. Comparison between plate  $\beta=0.5$  and plate  $\beta=0.38$ , turbulence intensity that has been generated by plate  $\beta=0.38$  is higher than plate  $\beta=0.5$  starting at the first point until the end.

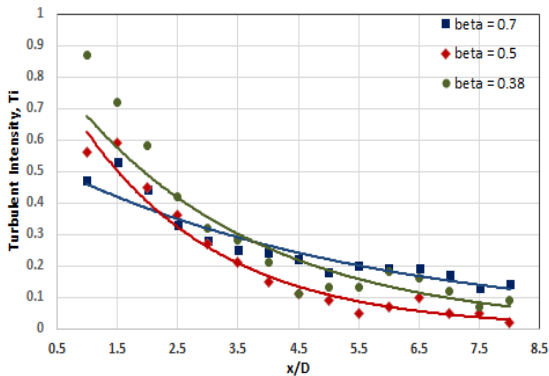


Fig. 4 - Turbulence intensity against  $x/D$  for Reynolds number 10625

Furthermore using air flow that has Reynolds number 9722 and the inlet velocity of air flow is 2.8 m/s. All of three graphs is parabolic curve. Based on the graph, at the first point  $x/D=1$  plate  $\beta=0.38$  generate higher turbulence intensity followed plate  $\beta=0.5$  and plate  $\beta=0.7$  that is 0.84, 0.58, and 0.52. For plate  $\beta=0.5$ , the highest turbulence intensity that it generate is 0.64 at  $x/D=2$ . Turbulence intensity that was generated by three plate decreases dramatically starting  $x/D=1$  to  $x/D=4$  and slowly decreases until reach constant turbulence intensity. At point  $x/D=2$ , turbulence intensity that had been generated by plate  $\beta=0.7$  and plate  $\beta=0.5$  is same that is 0.36. While at point  $x/D=3.4$  turbulence intensity that had been generated by plate  $\beta=0.7$  and plate  $\beta=0.38$  is same that is 0.26. At the last point  $x/D=8$ , plate  $\beta=0.7$  generate higher turbulence intensity than plate  $\beta=0.38$  and plate  $\beta=0.5$  that is 1.2, 0.8, and 0.5.

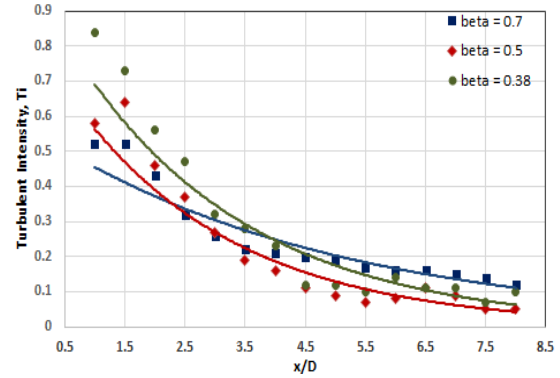


Fig. 5 - Turbulence intensity against  $x/D$  for Reynolds number 9722

Next, Reynolds number 8819 was used to identify turbulence intensity that can generated. Fig. 6 shows relationship between turbulence intensity and  $x/D$  for three plates that have different porosity. From point  $x/D=1$  to  $x/D=4$ , the value of turbulence intensity decreases dramatically and then decreases slowly until it constant. Initially plate  $\beta=0.38$  generate highest turbulence intensity than plate  $\beta=0.5$  and plate  $\beta=0.7$  that is 0.95, 0.7, and 0.54. But, for plate  $\beta=0.5$  the highest turbulence intensity is achieved at point  $x/D=2$  that is 0.72. Start point  $x/D=4$  until point  $x/D=8$ , turbulence intensity that had been generated by plate  $\beta=0.5$  and plate  $\beta=0.38$  is the same. While at point  $x/D=3.6$ , all of plate generate same turbulence intensity that is 0.24 and the next, plate  $\beta=0.7$  generate higher turbulence intensity than plate  $\beta=0.5$  and plate  $\beta=0.38$ . At last point  $x/D=8$ , plate  $\beta=0.5$  and plate  $\beta=0.38$  generate 0.8 turbulence intensity and plate  $\beta=0.7$  generate 0.12.

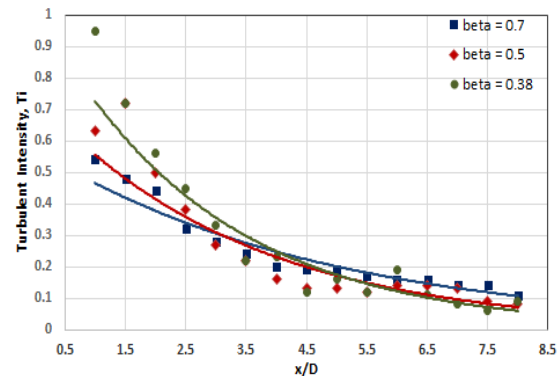


Fig. 6 - Turbulence intensity against  $x/D$  for Reynolds number 8819

For the minimum Reynolds number 7917, the inlet velocity flow of air is 2.28 m/s. Fig. 7 shows the graph parabolic curve. Its means turbulence intensity that had been generated by fractal plate is decreases when it farther away from the plate. Based on the graph, turbulence intensity is decreases dramatically from starting plate until point  $x/D=4$ . At this range, the highest turbulence intensity that had been generated is 0.86 from plate  $\beta=0.38$ . When  $x/D=3$ , plate  $\beta=0.7$  and plate  $\beta=0.5$  generate same value turbulence intensity that is 0.26. At position  $x/D=5.6$ , plate  $\beta=0.7$  and plate  $\beta=0.38$  generate same turbulence intensity that is 0.14. At the last point  $x/D=8$ , plate  $\beta=0.7$ , B, and C generate 0.1, 0.8, and 0.6 turbulence intensity.

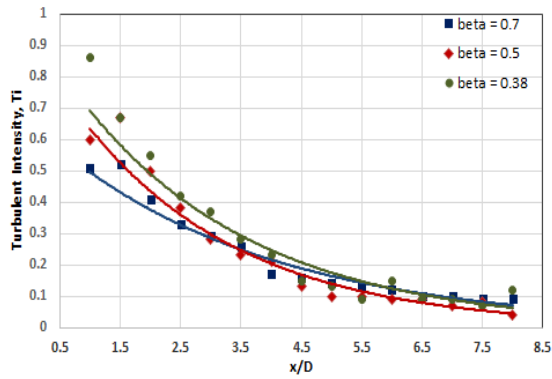


Fig. 7 - Turbulence intensity against  $x/D$  for Reynolds number 7917

#### 4.2 Summary of Turbulence Intensity based on Different Reynolds Number

Based on all graph with different Reynolds number was plotted, the graph is parabolic curve. Its means turbulence intensity will decreases when it keeps away from the fractal plate. The graph shows the value of turbulence intensity that had been generated from different Reynolds number is look like same for every point. From point  $x/D=1$  to  $x/D=4$  all graphs shows the turbulence intensity decreases dramatically and then decreases slowly until it achieved constant value. At the first point  $x/D=1$ , the highest turbulence intensity generated is 0.95 by plate  $\beta=0.38$  at Reynolds number 8819. While the lowest turbulence intensity was generated is 0.52 by plate  $\beta=0.7$  at Reynolds number 9722. At range  $x/D=1$  until  $x/D=4.5$ , plate  $\beta=0.38$  generated higher turbulence intensity than plate  $\beta=0.7$  and  $\beta=0.5$ . But at range  $x/D=4.5$  until  $x/D=8$ , plate  $\beta=0.7$  generate turbulence intensity higher than plate  $\beta=0.38$  and  $\beta=0.5$  and the highest value that it can reached is 0.13 at point  $x/D=8$  for Reynolds number 10625. For comparison between plate  $\beta=0.38$  and plate  $\beta=0.5$ , turbulence intensity that had been generated by plate  $\beta=0.38$  is higher than plate  $\beta=0.5$  from point  $x/D=1$  until  $x/D=8$ .

So in conclusion, if the distance between turbulence generator and combustion chamber is lower than  $x/D=4.5$ , fractal plate with porosity 14.45% is suitable to used for combustion if the value of turbulence intensity that can be generated from that plate matching with the aspect combustion needed. If the distance between turbulence generator and combustion chamber is more than  $x/D=4.5$  until  $x/D=8$ , fractal plate with porosity 51.85% is suitable to used.

#### 4.3 Turbulence Intensity for Various Porosity Plates

In this experiment, three plates are used to measure and identify turbulence intensity that can be generated using air test rig. Three of the plates have different porosity that is 14.45% (0.38 blockage ratio), 25% (0.5 blockage ratio), and 51.85% (0.7 blockage ratio). Every plate is estimated can be disturb the flow of air and become turbulence flow and will generate different turbulence intensity at different point. In this section will discuss about relationship between turbulence intensity that had been generated at different Reynolds number.

For plate  $\beta=0.7$ , the porosity plate is 51.85%. Fig. 8 shows the graph is parabolic curve. Turbulence intensity decreases when the measurement farther away from the plate. Figure 4.6 also shows turbulence intensity that had been generated by five different Reynolds number. Based on the graphs, the value of turbulence intensity at each point is quite different with different Reynolds number. Initially graph shows turbulence intensity was decreases dramatically from  $x/D=1$  to  $x/D=4$  and

then decreases slowly until it achieved constant turbulence intensity. At initial point  $x/D=1$ , the highest and lowest turbulence intensity generated at Reynolds number 7916 and 11528 that is 0.72 and 0.52. Reynolds number 7916 generated turbulence intensity higher than others start from  $x/D=1$  to  $x/D=1.8$  and the next Reynolds number 10625 generated higher turbulence intensity than other until  $x/D=8$ . At the end point, the highest and lowest turbulence intensity is 0.15 and 0.09 generated by Reynolds number 10625 and 7916.

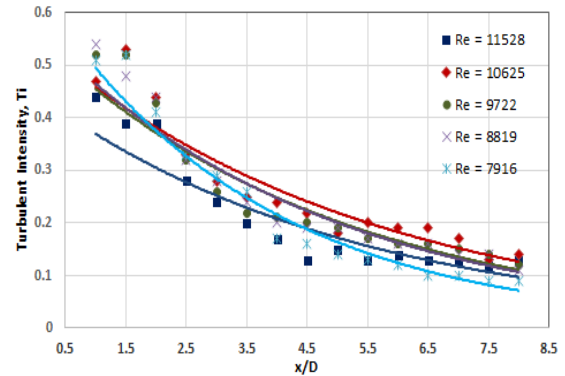


Fig. 8 - Turbulence intensity against  $x/D$  for plate  $\beta=0.7$

Next plate, the blockage ratio is  $\beta=0.5$  and the porosity is 25%. Figure 4.7 shows relationship between turbulence intensity with porosity plate at different Reynolds number. In range  $x/D=1$  to  $x/D=2$ . The lowest Reynolds number that is 7919 generates higher turbulence intensity than others. While in range  $x/D=2$  until the end, turbulence intensity is higher generated by Reynolds number 8819. At the end point, the highest turbulence intensity is 0.1.

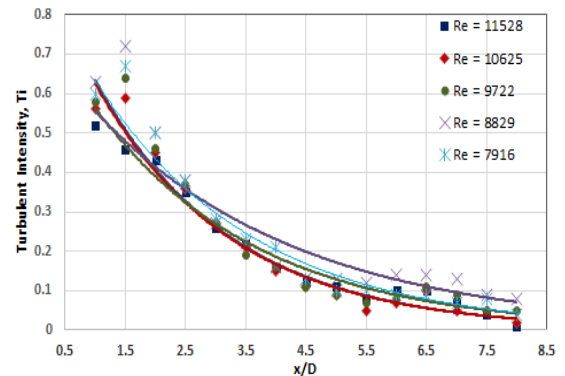


Fig. 9 - Turbulence intensity against  $x/D$  for plate  $\beta=0.5$

The last plate is 0.38 blockage ratio and 14.45% porosity. Figure 4.8 shows all graphs is in a line. Its means turbulence intensity that had been generated by all Reynolds number at each point is same. Based on the graph, turbulence intensity decreases dramatically at point  $x/D=1$  to  $x/D=4$  and then it decreases slowly until it reach constant turbulence intensity. At point  $x/D=8$ , the highest turbulence intensity is 0.08.

Based on three graph was plotted, it can see that turbulence intensity decreases when it farther away from the plate. In range  $x/D=1$  to  $x/D=4$ , the value of turbulence intensity decreases dramatically and then it decreases slowly. If make a comparison between three graph was plotted at initially point, turbulence intensity that had been generated by large porosity 51.85% is lower than plate porosity 25% and plate porosity 14.45%. But, if the distance from plate is farther, turbulence intensity that had been generated by large porosity plate 51.85% is higher than porosity plate 25% and porosity plate 14.45%.

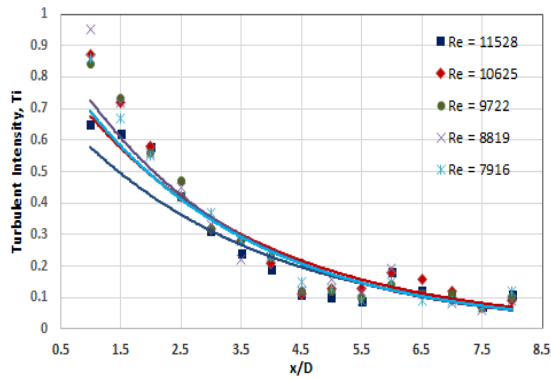


Fig. 10 - Turbulence intensity against  $x/D$  for plate  $\beta=0.38$

#### 4.4 Pressure Drop across Fractal Plate

A good flow conditioner should have not only a good performance in dampening the disturbances but also a minimum pressure loss as well. Pressure difference between  $1D$  and  $1D$  upstream and downstream of the flow conditioner was measured. The results of these tests were plotted in Figure 4.9 for air test rig. The left-hand ordinate is the actual pressure drop measured in the experiment. As expected, the fractal plate, having high porosity, generated a low pressure drop (as low as 280 Pa at high Reynolds number). While the fractal plate having low porosity generated high pressure although at low Reynolds number.

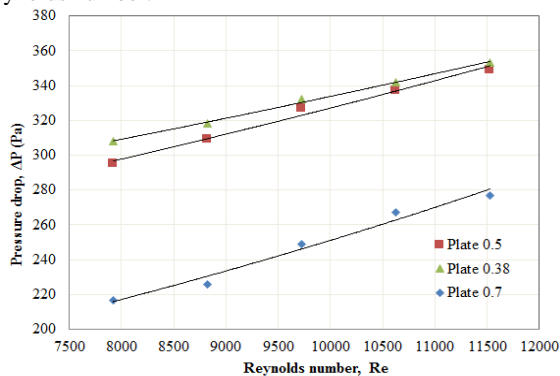


Fig. 10 - Pressure drop,  $\Delta P$  against the Reynolds number

#### 5. Conclusions

For the conclusion, all of the fractal pattern that used in this research effective to generate turbulence flow. The turbulence flow can be measured by measure the velocity of the air flow after through the fractal plate at multiple-point. But, the value of turbulence flow is different following the porosity of plate. Three of the plate was compared and obtained that plate with higher porosity (51.85%) was generate low turbulence intensity at nearly downstream. Otherwise, in range  $1D$  to  $4.5D$  the plate with low porosity (14.45%) was generate higher turbulence intensity than others plate. But, the turbulence intensity was decreases dramatically at that range. Different with plate higher porosity which is, although it generated low turbulence in short distance downstream but it decreases slowly until large distance downstream. At the large distance downstream ( $8D$ ), plate with higher porosity was generate higher turbulence intensity than others plate. When comparison between plate with low porosity (14.45%) and medium porosity (25%) is made, it found that plate with low porosity can generate higher turbulence intensity in all range ( $1D$  to  $8D$ ).

10

In this study, plate with low porosity is better to generate turbulence intensity in range  $1D$  to  $4.5D$  near to downstream and in range  $4.5D$  to  $8D$ , plate higher porosity is better to generate turbulence intensity. So, a combustion system can select which one plate better based on distance between turbulence generator and combustion chamber to produce high efficiency combustion.

#### Acknowledgement

The authors thank the EMFA Industry Sdn Bhd and Nukilan Gemilang Sdn Bhd for the support on ongoing for this project and also for Aeronautical Laboratory, UTHM for support on experimental and validation work.

#### References

- [1] D.P. Mishra. (2004). Emission studies of impinging premixed flames. *Fuel*, 83, pp. 1743–1748.
- [2] Shengteng, H., Peiyong, W., & Robert, W. P. (2009). A structural study of premixed tubular flames. *Proceedings of the Combustion Institute*, 32, pp. 1133–1140.
- [3] Silva, A. L. F. de L. e, Silva, A. R. da, & Silveira Neto, A. da. (2007). Numerical simulation of two-dimensional complex flows. *Journal of the Brazilian Society of Mechanical Sciences and Engineering*, 29(4), 379–387.
- [4] M. F. Othman, B. Manshoor and A. Khalid (2013). Circle grid fractal plate as a turbulent generator for premixed flame: An overview. Paper presented at the IOP Conference Series: Materials Science and Engineering.
- [5] M. Kearney (1997). Engineered fractal cascades for fluid control applications, *Fractals in Engineering Proceedings*. Arcachon, France.
- [6] B. Mazzi, F. Okkels and J. Vassilicos (2002). A shell-model approach to fractal induced turbulence. *European Physical Journal*, p. 243-251.
- [7] Aly, A.A.E.-A. 2008). Study of the dispersion of heavy-particle sets in turbulent flows and of the fractal geometry of heavy-particle line using Kinematic Simulation to enhance Fluid Power Systems, in *Mechanical Engineering*. Sheffield University: Sheffield.